


Research Article

The molecular chaperone β -casein prevents amorphous and fibrillar aggregation of α -lactalbumin by stabilisation of dynamic disorder

Henry M. Sanders¹, Blagojce Jovcevski¹, John A. Carver² and  Tara L. Pukala¹

¹School of Physical Sciences, The University of Adelaide, Adelaide, SA 5005, Australia; ²Research School of Chemistry, Australian National University, Acton, ACT 2601, Australia

Correspondence: Tara L. Pukala (tara.pukala@adelaide.edu.au)



Deficits in protein homeostasis (proteostasis) are typified by the partial unfolding or misfolding of native proteins leading to amorphous or fibrillar aggregation, events that have been closely associated with diseases including Alzheimer's and Parkinson's diseases. Molecular chaperones are intimately involved in maintaining proteostasis, and their mechanisms of action are in part dependent on the morphology of aggregation-prone proteins. This study utilised native ion mobility–mass spectrometry to provide molecular insights into the conformational properties and dynamics of a model protein, α -lactalbumin (α -LA), which aggregates in an amorphous or amyloid fibrillar manner controlled by appropriate selection of experimental conditions. The molecular chaperone β -casein (β -CN) is effective at inhibiting amorphous and fibrillar aggregation of α -LA at sub-stoichiometric ratios, with greater efficiency against fibril formation. Analytical size-exclusion chromatography demonstrates the interaction between β -CN and amorphously aggregating α -LA is stable, forming a soluble high molecular weight complex, whilst with fibril-forming α -LA the interaction is transient. Moreover, ion mobility–mass spectrometry (IM-MS) coupled with collision-induced unfolding (CIU) revealed that α -LA monomers undergo distinct conformational transitions during the initial stages of amorphous (order to disorder) and fibrillar (disorder to order) aggregation. The structural heterogeneity of monomeric α -LA during fibrillation is reduced in the presence of β -CN along with an enhancement in stability, which provides a potential means for preventing fibril formation. Together, this study demonstrates how IM-MS and CIU can investigate the unfolding of proteins as well as examine transient and dynamic protein–chaperone interactions, and thereby provides detailed insight into the mechanism of chaperone action and proteostasis mechanisms.

Introduction

Globular proteins rely on the formation of discrete, low-energy, three-dimensional native structures in order to carry out their biological function [1]. As newly synthesised proteins are produced, they undergo an 'on-pathway' folding process to the native state, involving condensation of hydrophobic residues into a non-solvent exposed core, while the remaining residues sample available structural conformations. The folding process is largely 'downhill', with successive structures being lower in energy with fewer degrees of freedom, thereby rapidly accelerating the process [1–3]. However, conditions of cellular stress can render proteins unable to adopt their native conformation, instead directing proteins towards 'off-pathway' folding mechanisms. Here, proteins populate partially unfolded, intermediate states which are prone to self-assembly through the formation of either amorphous aggregates or amyloid fibrils [4,5]. Amorphous aggregates form due to random hydrophobic associations between misfolded proteins that become insoluble after reaching a critical aggregate size [6]. In

Received: 2 September 2019
Revised: 10 January 2020
Accepted: 15 January 2020

Accepted Manuscript online:
15 January 2020
Version of Record published:
11 February 2020

contrast, fibril formation results from a nucleated growth process whereby ordered monomeric units stack perpendicularly to the fibril axis, forming a cross- β -sheet structure. Multiple resultant ‘protofibril’ strands assemble to produce mature fibrils [7–9].

Molecular chaperones are a crucial constituent of the protein quality control network which regulates protein refolding, stabilisation, sequestration and degradation. Failure of this protein quality control network propagates the formation of misfolded and aggregation-prone proteins which are implicated in disease [10,11]. For example, Alzheimer’s and Parkinson’s diseases are two of the many disorders associated with the formation of amyloid fibrils [4]. Amorphous aggregates are considered non-toxic, with nuclear cataracts being the most notable amorphous aggregate-associated disease [12]. To date, there are no effective therapeutic approaches to treat neurodegenerative diseases in which misfolding proteins are implicated. Understanding distinctions between these off-folding pathways can allow for more effective therapeutic design, for example by redirecting misfolded proteins from a fibrillar to an amorphous pathway *in vivo*. Therefore, a robust model misfolding protein that is able to mimic physiologically relevant conditions and follow both amorphous and fibrillar aggregation pathways is a valuable tool for assessing potential inhibitors of protein aggregation.

Bovine α -lactalbumin (α -LA) is a 14.2 kDa acidic calcium-binding milk protein which plays an essential role in the biosynthesis of lactose within the mammary glands [13]. The protein consists of a large α -helical domain, a small β -sheet domain and a calcium-binding loop, a conformation which is stabilised by four disulfide bonds [14]. α -LA undergoes amorphous aggregation when reduced with dithiothreitol (DTT α -LA), but forms fibrillar aggregates when reduced and carboxymethylated (RCM α -LA) due to formation of a partially folded intermediate state [15–18]. As a result, α -LA is a useful system for investigating structural distinctions between amorphous and fibrillar aggregation, and identifying which conformations dictate these aggregation pathways. β -casein (β -CN) is an intrinsically disordered major milk protein [19] which has a monomer mass of ~24 kDa, and at temperatures above ~20°C, forms concentration-dependent oligomers known as micelles [20]. Like the other bovine caseins, β -CN exhibits chaperone activity to prevent the unfolding and amorphous aggregation of proteins under stress conditions such as elevated temperature [21]. β -CN also prevents amyloid fibril formation of κ -casein [22–24].

Difficulties associated with investigating the mechanisms of chaperone-mediated proteostasis and characterising the transient interactions between chaperones and aggregation-prone proteins mean that a combination of biophysical techniques is required to probe this process. Native mass spectrometry (MS) is well-suited for the analysis of protein–protein interactions, given the gentle nature and low sample requirements of nano-electrospray ionisation. MS enables the preservation and interrogation of low-abundant, heterogeneous assemblies formed during aggregation. When paired with ion mobility (IM), ion mobility–mass spectrometry (IM-MS) allows the size, stoichiometry and dynamics of protein assemblies to be studied. Moreover, the unfolding dynamics of proteins can be observed by gas-phase manipulation through collision-induced unfolding (CIU), enabling the measurement of protein stability and protein–protein interactions in the gas-phase, all of which are reflective of their solution-phase properties [25–29].

To understand the structural features that direct α -LA towards either the amorphous or fibrillar aggregation pathways, we utilised an integrated biophysical approach to observe the differences in monomeric α -LA structure and stability following chemical modification (i.e. reduction via DTT to give DTT α -LA compared with RCM α -LA). In addition, we have assessed the ability of β -CN to inhibit amorphous and fibrillar aggregation of DTT α -LA and RCM α -LA, respectively. In particular, IM-MS was implemented to probe changes in the conformation and unfolding dynamics of α -LA, and CIU was used to understand better the effects of β -CN in protecting against aggregation through stabilisation of α -LA monomers. Identifying distinct changes in conformation and dynamics that dictate which aggregation pathway proteins follow, as well as their interaction with molecular chaperones, provides a greater understanding of how chaperones arrest protein unfolding, misfolding and aggregation. Moreover, this study highlights how MS-based approaches can be utilised to probe transient and highly dynamic protein–protein interactions.

Experimental procedures

Bovine α -LA (type II, calcium-depleted, 85% pure, lyophilised), β -CN and all other reagents were purchased from Sigma–Aldrich (St. Louis, U.S.A.) unless stated otherwise. DTT was obtained from Astral Scientific (GyMEA, Australia). Reduction and carboxymethylation (RCM) of α -LA was performed as described previously [30] and confirmed by observation of the associated mass increase using MS (Supplementary Figure S1). RCM

α -LA was buffer exchanged into ammonium acetate (100 mM) using an Amicon Ultra-4 centrifugal spin filter at 4°C. Samples were lyophilised and stored at –80°C until use.

Amorphous and fibrillar aggregation assays

The DTT-induced (2 mM final concentration) amorphous aggregation of α -LA (DTT α -LA; 100 μ M) was monitored by the change in light scattering at 340 nm. Aggregation of α -LA was performed in 100 mM ammonium acetate (pH 7.0) in the absence and presence of β -CN at various molar ratios (1 : 1, 1 : 10 and 1 : 100, β -CN : DTT α -LA). Amorphous assays were plated (200 μ l/well) into sealed 96-well microplates (Greiner Bio-One) and aggregation was monitored using a FLUOstar Optima microplate reader (BMG Lab Technologies, Melbourne, Australia) over a period of 6 h at 37°C, with an initial shaking period of 300 s. Fibrillar aggregation of RCM α -LA was monitored in real-time using a ThT fluorescence assay [15]. Fibrillation of RCM α -LA was performed in 100 mM ammonium acetate (pH 7.0) in the absence and presence of β -CN at various molar ratios (1 : 1, 1 : 2, 1 : 10, 1 : 20 and 1 : 100, β -CN : RCM α -LA). Fibrillar assays were plated (50 μ l/well) into sealed 384-well microplates (Greiner Bio-One) and fibril formation was monitored using a FLUOstar Optima microplate reader (BMG Lab Technologies, Melbourne, Australia) over a period of 24 h at 37°C with shaking (double orbital, 50 rpm) for 30 s prior to fluorescence measurement. ThT fluorescence was measured using an excitation and emission wavelength of 440 and 490 nm, respectively. All assays were performed in triplicate and reported as mean \pm SEM. The degree of inhibition (%) afforded by β -CN against amorphous and fibrillar aggregation was calculated as described previously [31].

Transmission electron microscopy

Three microliters of sample was taken immediately at the conclusion of the light scattering or ThT assay and placed directly onto a carbon-coated 400-mesh nickel TEM grid (ProSciTech, Thuringowa Central, Australia) [32]. Grids were washed with 0.22 μ m filtered MilliQ water and stained with 2% (w/v) uranyl acetate solution. Samples were viewed using either a CM100 transmission electron microscope (Philips, Eindhoven, Netherlands) or a Tecnai G2 Spirit TEM (FEI, Oregon, U.S.A.) with a magnification of 45 000 \times .

Intrinsic tryptophan and bis-ANS fluorescence

Both intrinsic tryptophan and bis-ANS fluorescence studies were performed using a Cary Eclipse fluorescence spectrophotometer (Varian Inc., Mulgave, Australia) at room temperature. Excitation and emission slit widths were adjusted to 2.5 nm and scan speed was set at 60 nm/min. Native α -LA, DTT α -LA and RCM α -LA (100 μ M) were prepared in 100 mM aqueous ammonium acetate (pH 7.0). Fluorescence was measured using a quartz cuvette of pathlength 1 cm. Intrinsic tryptophan fluorescence was measured using an excitation wavelength of 295 nm and emission was measured from 300 to 400 nm. To determine the exposed hydrophobicity of all α -LA forms, 4,4'-dianilino-1,1'-binaphthyl-5,5'-disulfonic acid (bis-ANS) (10 μ M) was added and fluorescence emission was measured from 400 to 600 nm following excitation at 385 nm. The obtained spectra represent the average of at least 3 scans.

Analytical size-exclusion chromatography

The interaction between α -LA and β -CN was observed by SEC [33]. Samples (100 μ M) following aggregation were centrifuged at 14 000 $\times g$ for 30 min at 4°C and subsequently loaded (500 μ l) onto a Superdex 200 10/300 GL analytical-SEC (GE Healthcare, Illinois, U.S.A.) which was equilibrated with 100 mM ammonium acetate (pH 7.0) at a flow rate of 0.4 ml/min at room temperature. The SEC column was calibrated using standards (Sigma–Aldrich, Missouri, U.S.A.) containing bovine thyroglobulin (670 kDa), bovine γ -globulin (158 kDa), chicken ovalbumin (44 kDa) and horse myoglobin (17 kDa).

SDS-PAGE

Eluted fractions following analytical-SEC were further examined by SDS-PAGE (12% gels) (Bio-rad, California, U.S.A.) and bands were visualised using a Silver staining kit (Invitrogen, California, U.S.A.) for analytical-SEC fraction analysis and Coomassie Brilliant Blue stain (ThermoFisher, Massachusetts, U.S.A.) for band density analysis. Both techniques were performed according to the manufacturer's instructions. Band densities were calculated using GelAnalyzer 9.1 (<http://www.gelanalyzer.com/>).

Ion mobility–mass spectrometry

The conformation of α -LA forms was investigated by IM-MS performed on a Synapt HDMS Q-TOF mass spectrometer (Waters Corporation, Manchester, U.K.) using a nano-electrospray ionisation source. Samples were prepared in 100 mM ammonium acetate (pH 7.0) to a final concentration of 25 μ M. DTT α -LA was formed by the addition of DTT (2 mM) and RCM α -LA was incubated in the presence of β -CN (1 : 0.5 molar ratio; RCM α -LA : β -CN). Samples were loaded into platinum-coated borosilicate glass capillaries prepared in-house. Gentle source conditions were applied to minimise gas-phase structural changes prior to detection, with instrument parameters as follows: capillary voltage, 1.60 kV; sampling cone, 30 V; extraction cone, 1.5 V; trap/transfer collision energy, 10/15 V; trap gas, 5.5 l/h; backing gas, \sim 4.5 mbar. The parameters for IM were as follows: IM cell wave height, 8 V; IM cell wave velocity, 350 m/s; transfer t-wave height, 8 V; transfer t-wave velocity, 250 m/s. Mass spectra and arrival time distributions (ATDs) were viewed using MassLynx (v4.1) and DriftScope (v2.1), respectively (Waters Corporation, Manchester, U.K.).

Collision-induced unfolding

The CIU dynamics of α -LA forms was investigated by observing the unfolding of the monomer⁷⁺ charge state (native α -LA at 2031 m/z and RCM α -LA at 2093 m/z) and IM spectra were collected under the conditions stated above. Unfolding of the monomer⁷⁺ ions was induced by increasing the trap collision energy (activation energy) by 2.5 V increments from 10 to 60 V. CIU heat maps were generated using CIUsuite with default parameters [34]. The proportion of unfolded α -LA with increasing activation energy was calculated by normalising the ATD to the highest intensity, taking the relative intensity of any unfolded species present as a function of folded α -LA [34,35]. A dose–response (sigmoidal) curve was applied to calculate the CIU₅₀ (i.e. the voltage at which 50% of the monomer as unfolded) and the rate of unfolding (denoted by the Hill slope of the sigmoidal fit). The equation is shown below:

$$y = \text{bottom} + \frac{(\text{top} - \text{bottom})}{1 + 10^{(\text{CIU}_{50} - x) \times \text{rate of unfolding}}}$$

where bottom and top refer to the bottom and top of the plateau, i.e. the folded and unfolded states of α -LA. Curve fitting analyses were performed using Prism 7.0 (GraphPad Software, San Diego, U.S.A.) software.

Results

β -CN is more effective at inhibiting RCM α -LA fibril formation compared with DTT-induced amorphous aggregation

To evaluate the ability of β -CN to inhibit both amorphous and fibrillar aggregation of α -LA, chaperone assays were performed at various α -LA : β -CN molar ratios (Figure 1). In the absence of β -CN, insoluble amorphous aggregates of α -LA (100 μ M) were induced upon addition of DTT (2 mM) in ammonium acetate (100 mM, pH 7.0), whereupon an increase in light scattering occurred at \sim 0.75 h and reached a plateau indicative of amorphous aggregate formation after \sim 2.5 h (Figure 1A, black), which was confirmed by TEM (Figure 1A, top inset). The lag-phase for DTT α -LA aggregation was unchanged in the presence of β -CN across all molar ratios (ranging from 1 : 1 to 100 : 1, DTT α -LA : β -CN), however, the subsequent rate and degree of light scattering decreased in a β -CN concentration-dependent manner (Figure 1C). β -CN exhibited intermediate ability at inhibiting the amorphous aggregation of α -LA with \sim 60% inhibition at a 1 : 1 ratio (DTT α -LA : β -CN) and no inhibition at 100 : 1 (Figure 1C). In addition, the activity of β -CN was not affected by the presence of DTT as no increase in light scattering was observed for the β -CN only control, consistent with its absence of disulfide bonds (Supplementary Figure S2).

The ability of β -CN to inhibit α -LA fibril formation was assessed using a ThT aggregation assay (Figure 1B,D). In the absence of β -CN, RCM α -LA (200 μ M) forms amyloid fibrils in ammonium acetate (100 mM, pH 7.0) as evidenced by an increase in ThT fluorescence from \sim 7.5 h, indicative of fibril elongation and maturation without the need for MgCl₂, which previous studies (in phosphate buffer) have used to promote fibril formation [15]. In addition, the formation of mature RCM α -LA fibrils was confirmed by TEM (Figure 1C, top inset). The efficiency of β -CN as a fibril inhibitor was apparent from these assays, whereby 1 : 1 and 100 : 1 molar ratios (RCM α -LA : β -CN) exhibited near total inhibition and \sim 33% inhibition, respectively (Figure 1D). In addition, near total inhibition was observed at a 2 : 1 molar ratio (RCM α -LA : β -CN) (Supplementary

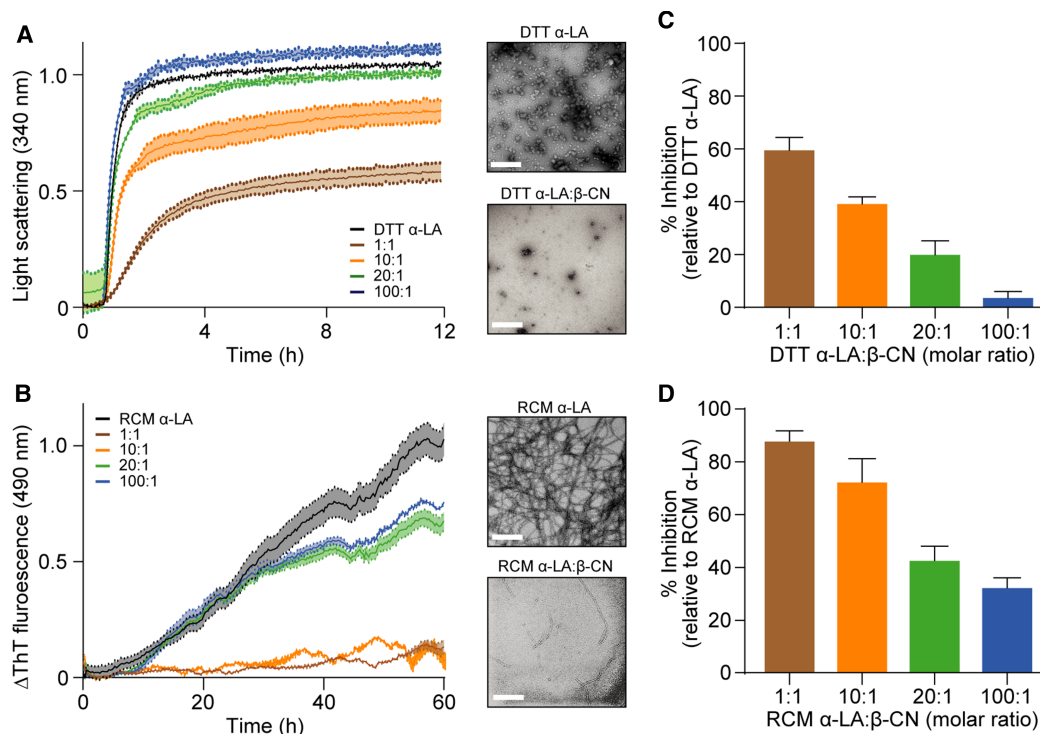


Figure 1. β -CN inhibits the amorphous and fibrillar aggregation of α -LA.

(A) DTT α -LA (100 μ M) amorphous aggregation was monitored by the change in light scattering at 340 nm. Aggregation was induced with DTT (2 mM) in ammonium acetate (100 mM, pH 7.0) in the presence of various β -CN molar ratios. TEM image (A, inset) displays the morphology of amorphous aggregates in the presence (1 : 1 molar ratio) and the absence of β -CN. (B) Fibril formation of RCM α -LA was monitored by the change in ThT fluorescence at 490 nm (excitation at 440 nm) at various molar ratios of β -CN to determine chaperone activity. A corresponding TEM image shows the morphology of RCM α -LA fibrils in the presence (1 : 1 molar ratio) and the absence of β -CN (B, inset). (C) The concentration-dependent chaperone activity of β -CN against amorphous aggregation was calculated by comparing the degree of light scattering at the conclusion of the assay. (D) The concentration-dependent chaperone activity of β -CN against fibril formation was calculated by comparing the degree of ThT fluorescence at the conclusion of the assay. Data are reported as mean \pm SEM ($n = 3$). Scale bars represent 400 μ m.

Figure S2). To ensure the ThT data accurately reflects the fibril yields, the relative amount of soluble material was assessed following the 72-h aggregation period using SDS-PAGE (Supplementary Figure S3). A clear decrease in monomeric RCM α -LA is observed following fibril formation, which is restored to a significant degree in the presence of β -CN. Overall, the data demonstrate the potent ability of β -CN to prevent α -LA aggregation, with much greater efficiency towards inhibiting fibril formation.

Previous work has suggested the major difference between the two α -LA states is due to carboxymethylation of α -LA, which adds additional negative charge to the protein and, because of repulsive interactions, induces the protein to adopt a more extended and flexible state capable of forming structural motif(s) that are prerequisite for fibril formation [16]. In contrast, reduced (DTT) α -LA adopts more rigid structures which lead to the formation of amorphous aggregates. Aggregation kinetics of the α -LA species is also a likely factor. Amyloid fibril formation is favoured over amorphous aggregation by slowly aggregating species, and Figures 1A,B, along with work by Kulig and Ecroyd [15], show that reduced (amorphously aggregating) α -LA aggregates at an earlier time point than (amyloid fibril-forming) RCM α -LA, i.e. the former has a shorter lag-phase.

Structural modifications of monomeric α -LA dictate its interaction with β -CN to prevent aggregation

To further probe the difference in the ability of β -CN to prevent amorphous and fibrillar aggregation of α -LA, a better understanding of the structural differences between monomeric α -LA forms is required. Intrinsic

tryptophan and extrinsic bis-ANS fluorescence studies were employed to probe the tertiary structure and exposed hydrophobicity of aggregation-prone forms of α -LA. RCM α -LA demonstrated a 250% increase in tryptophan fluorescence compared with native α -LA, whilst DTT α -LA displayed only a 60% increase in fluorescence (Figure 2A). In addition, RCM α -LA displayed a large fluorescence red-shift (29 nm shift to 354 nm) compared with native α -LA (absorbance maxima at 325 nm) which was less prevalent for DTT α -LA with only a 17 nm red-shift to 342 nm (Figure 2A). In contrast, the dye bis-ANS, which monitors clustered exposed hydrophobicity of a protein, showed a fluorescence increase in 85% for DTT α -LA compared with RCM α -LA which only exhibited a 20% increase in fluorescence (Figure 2B). A control sample was also analysed to ensure that the excess DTT did not affect tryptophan fluorescence (Supplementary Figure S4). In contrast, the hydrophobic residues of DTT α -LA are more exposed to solvent compared with RCM α -LA and the tryptophan residues are more shielded, which is consistent with the protein adopting an intermediately folded, ‘molten globule’ state as previously reported [15,17,36].

From these fluorescence experiments, it is concluded that overall RCM α -LA exposes more of its four tryptophan residues to solvent due to unfolding than DTT α -LA whilst shielding hydrophobic residues. The observation in Figure 2B that DTT α -LA has greater ANS fluorescence than RCM α -LA is consistent with the general features adopted by both these forms of α -LA, i.e. RCM α -LA has a relatively extended (unfolded) conformation compared with DTT α -LA which adopts a more compact, molten globule structure that exposes the protein’s hydrophobic core to solution, and therefore binds ANS readily. Amorphous aggregates are formed much faster than amyloid fibrils and DTT α -LA exposes more hydrophobicity. RCM α -LA exposes less hydrophobicity, despite being less ordered than native α -LA. This may be important for the prerequisites for following a fibril formation pathway rather than amorphous aggregation pathway.

Analytical-SEC was performed in order to determine the nature of the interaction between α -LA and β -CN under the same conditions used for both aggregation assays and MS (Figure 2C,D). In their native states, β -CN and α -LA each eluted as a single peak of \sim 30 kDa in mass (13.5 ml) and 15 kDa in mass (17.2 ml), respectively (Figure 2C,D), consistent with their monomeric state. Prior to aggregation, DTT α -LA eluted as two, broad overlapping peaks (15.0 and 17.2 ml) indicative of monomeric α -LA and potentially low-molecular mass aggregates (e.g. dimer) (Figure 2C, purple). Importantly, the amount of soluble DTT α -LA decreased after aggregation with a small peak at \sim 670 kDa indicative of aggregated α -LA (Figure 2C, red). In the presence of an equimolar ratio of β -CN, the intensity of the peak \sim 8 ml (\sim 670 kDa) increased drastically corresponding to a high molecular weight (HMW) complex (Figure 2C, blue) containing both α -LA and β -CN, as determined by SDS-PAGE (Figure 2E). In the absence of β -CN, RCM α -LA eluted as a single peak at \sim 15.8 ml before (Figure 2D, purple) and after (Figure 2D, red) incubation. In contrast with DTT α -LA, RCM α -LA in the presence of β -CN does not form a HMW complex as no peak was observed at earlier elution volumes (Figure 2D, blue). The data suggest that the interaction between DTT α -LA and β -CN leads to stable complex formation between the two proteins in order to prevent amorphous aggregation, whilst β -CN interacts with RCM α -LA transiently in order to inhibit fibril formation.

IM-MS reveals conformational transitions of monomeric DTT and RCM α -LA during early stages of aggregation

Native IM-MS allows for the gentle separation of proteins in the gas-phase based on both mass to charge ratio (m/z) and rotationally averaged size (or collisional cross section), the latter of which can be monitored as a function of changes in solution properties or gas-phase activation and unfolding, providing conformational insight (Supplementary Figure S5). IM-MS was utilised here to observe conformational transitions of DTT and RCM α -LA monomers during their initial stages of aggregation. The most prominent peak for both DTT and RCM α -LA was the monomer⁷⁺ charge state (M^{7+}) at m/z 2031 (Figure 3A, red box). From this charge state, we extracted the ATD, providing information on the mobility of the ion through a buffer gas, which is dependent upon the protein’s three-dimensional structure. The ATD of the M^{7+} for DTT and RCM α -LA was analysed during the lag-phase of aggregation. Initially, the ATD of RCM α -LA M^{7+} exhibits two populations (at 5.8 and 8.1 ms) indicative of a predominantly compact (Figure 3B, blue box) and an unfolded state, respectively (Figure 3B, green box). The presence of the disordered state diminished during incubation, eventually disappearing after 2 h (Figure 3B). This trend was present for every major charge state, showing either an increase in compact structural populations, or a decrease in less compact populations (Supplementary Figure S6). In contrast, the presence of the unfolded state became more apparent in DTT α -LA during incubation after 1 h,

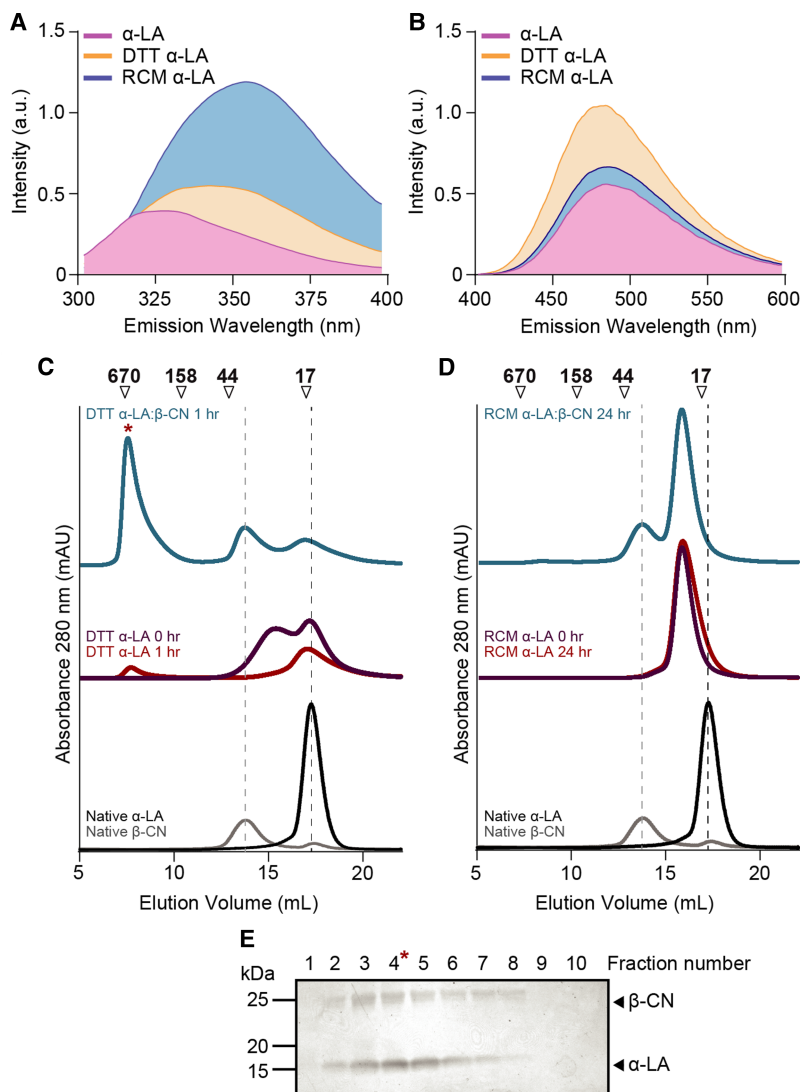


Figure 2. Structural modification of α -LA influences its interaction with β -CN.

(A) Intrinsic tryptophan fluorescence spectra of α -LA forms (100 μ M) in 100 mM ammonium acetate (pH 7.0), exhibiting an increase in tryptophan exposure for DTT- and RCM α -LA relative to native α -LA. (B) bis-ANS (10 μ M) fluorescence spectra measuring the clustered, exposed hydrophobicity of α -LA forms demonstrates an increase in exposed hydrophobicity for modified α -LA compared with native α -LA. (C) Analytical-SEC profiles of native α -LA (100 μ M) and β -CN (100 μ M). DTT α -LA (100 μ M) at 0 h (purple) and 1 h (red) post-incubation at 37°C was compared with DTT α -LA in the presence of β -CN (100 μ M, blue) forming a HMW complex (asterisk). Analytical-SEC experiments were performed in 100 mM ammonium acetate (pH 7.0). (D) Analytical-SEC profiles RCM α -LA (100 μ M) at 0 h (purple), 24 h (red) post-incubation at 37°C was compared with RCM α -LA in the presence of β -CN (100 μ M, blue). SEC experiments were performed in 100 mM ammonium acetate (pH 7.0) and elution volumes of molecular mass standards (kDa) are indicated above the chromatogram. (E) SDS-PAGE and silver staining of eluate fractions across the HMW peak from analytical-SEC of DTT α -LA in the presence of β -CN after 1 h of incubation. The asterisk indicates the fraction number (4) corresponding to the apex of the HMW peak.

despite hardly being present initially (Figure 3C). The ATDs of M^{7+} DTT and RCM α -LA were overlaid with the ATDs of their respective monomers at high and low activation energies (Supplementary Figure S7) to highlight that they are unfolded forms of the same species. RCM α -LA also showed a reduction in highly charged species indicating a compaction of structure, shielding residues from ionisation [37]. After incubation, DTT α -LA showed an increase in highly charged species indicative of unfolding (Supplementary Figure S8). Overall,

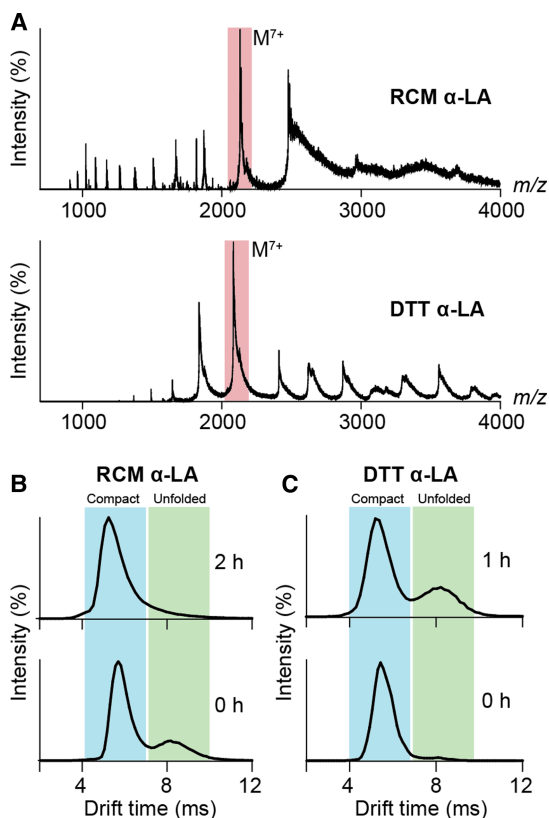


Figure 3. DTT and RCM α -LA undergo contrasting conformational transitions during the early stages of aggregation. (A) Native MS of RCM (top panel) and DTT α -LA (bottom panel) (both 25 μ M) at 0 h with the M^{7+} (m/z 2031) being the most abundant ion and selected for ATD analysis (red box). ATD of RCM (B) and DTT α -LA (C) M^{7+} during incubation at 37°C with shaking (300 rpm). The emergence of a disordered (unfolded) state (green box) during incubation of DTT α -LA contrasts to the disorder to order transition of RCM α -LA monomers during aggregation.

the data demonstrate that α -LA monomers follow disorder to order transitions (or vice versa) during initial stages of aggregation that is dependent on the aggregation pathway (i.e. amorphous or amyloid fibrillar).

IM-MS reveals differences in the conformation and unfolding propensity of RCM α -LA compared with native α -LA

The conformation and gas-phase unfolding dynamics of native and RCM α -LA in the absence and presence of β -CN were further examined by native IM-MS. The oligomeric state of native α -LA is predominantly monomeric with the M^{7+} charge state most prominent (Figure 4A, red box), as well as a population of dimer (D) (Figure 4A, top). RCM α -LA is also monomeric with a proportion of highly charged, unfolded monomer present (due to the increased exposure of ionisable residues as a result of its unfolded nature [37]) (Figure 4A, green box). A similar mass spectrum was also observed for RCM α -LA in the presence of β -CN, with both folded and unfolded monomeric RCM α -LA species present as well as monomeric β -CN (Figure 4A, bottom). The large proportion of highly charged monomeric signals indicative of unfolded RCM α -LA and lack of signals from oligomeric species evident in these spectra support the idea that the larger structures observed for RCM α -LA by SEC (Figure 2D) are extended, non-native states rather than higher-order aggregates.

To qualitatively probe the conformation and unfolding dynamics of α -LA, the ATD of the α -LA M^{7+} ions at 2031 m/z was monitored at low and high activation energy in the trap collision cell, allowing for resolution of folded (10–15 V) and unfolded (35–40 V) states (Figure 4B). Aside from being the most prominent charge state, the M^{7+} was chosen for IM-MS analyses in order to minimise charge state overlap from larger species (e.g. dimers) and was confirmed to be appropriate according to a power calculation which identifies suitable charge states for analysis [38]. The ATD for each folded and unfolded state also reflects the degree of heterogeneity within each

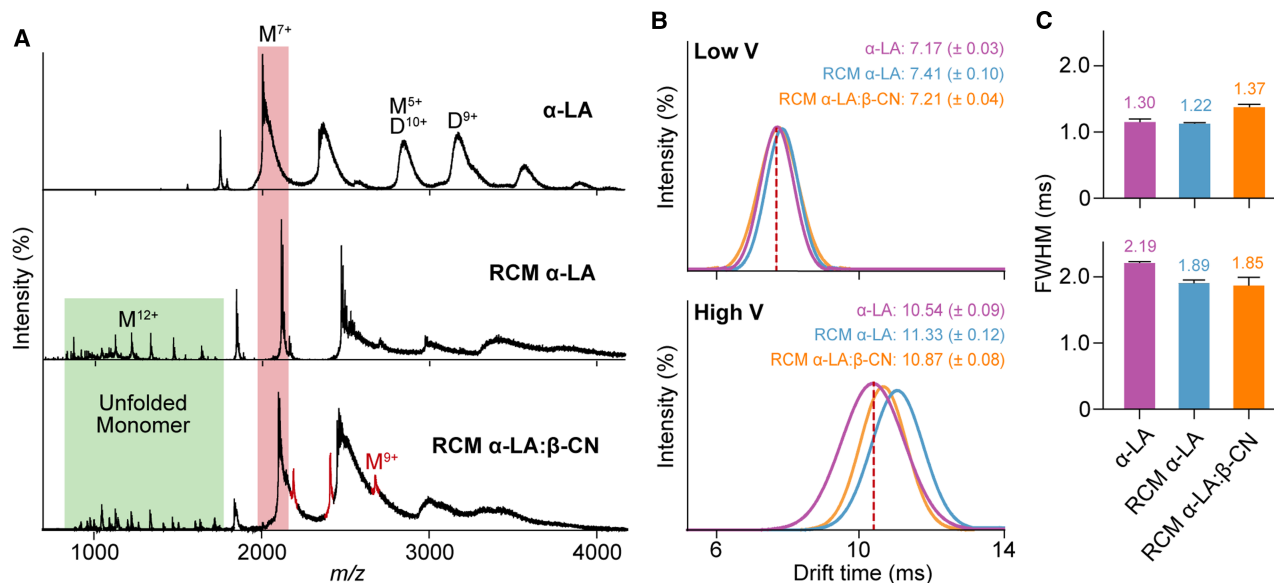


Figure 4. IM-MS analysis of native and RCM α -LA reveals differences in structure and dynamics with β -CN.

(A) Native MS of α -LA (top panel), RCM α -LA in the absence (middle panel) and presence (bottom panel) of β -CN (red) at a molar ratio of 2 : 1 (RCM α -LA : β -CN) after 15 min (final α -LA concentration, 25 μ M). MS reveals a slight shift in mass due to the RCM of α -LA as well as the presence of unfolded monomer (green box). The M^{7+} (orange box) was selected for IM-MS and subsequent CIU analysis. (B) ATDs of the M^{7+} of α -LA forms under low (10–15 V, top panel) and high (35–40 V, bottom panel) activation energy. (C) FWHM time for α -LA M^{7+} ATDs at low (10 V, top panel) and high (40 V, bottom panel) activation energy. States (monomer: M, dimer: D) are indicated with charge state in superscript. Data in B and C are reported as mean \pm SEM ($n = 3$).

population as represented by the full-width half maximum (FWHM) (Figure 4C). A larger FWHM indicates a more dynamic state that is sampling more conformations across a broader ATD, whereas a small FWHM indicates the ions adopt a relatively limited set of conformations. It should be noted that DTT α -LA was not similarly amenable to CIU studies due to the short time scale of amorphous aggregation preventing its analysis [17].

Under low activation energy, the ATD of all α -LA forms examined (native α -LA, RCM α -LA and RCM α -LA : β -CN) do not differ, with the exception that β -CN induced a slight broadening in the ATD for RCM α -LA compared with native and RCM α -LA alone (Figure 4B,C, top). Under high activation energy, however, changes in the ATD amongst α -LA forms were far more apparent, whereby RCM α -LA adopts a larger size compared with native α -LA as evidenced by a shift in the centroid of ATD to longer drift times (Figure 4B, bottom). Interestingly, this unfolding is somewhat attenuated in the presence of β -CN (Figure 4B, bottom). In addition, the conformational heterogeneity of RCM α -LA in the presence and absence of β -CN is reduced compared with native α -LA under high activation energy (Figure 4C, bottom). The data demonstrate that RCM α -LA unfolds more readily than native α -LA and that the presence of β -CN alters the structure of RCM α -LA, making it more native-like during activation.

β -CN enhances the stability of RCM α -LA monomers

We sought to quantitatively measure the stability RCM α -LA in the absence and presence of β -CN in the gas-phase by performing CIU IM-MS. Increasing activation (at increments of 2.5 V in the collision cell) of specific ions gradually shifted the ATD, allowing the stability and interconversion of individual species (i.e. folded to unfolded conformers) to be monitored (Figure 5A). Across all samples examined only two distinct populations were observed, even following extremely high activation up to 150 V, corresponding to folded and unfolded conformations, with a single unfolding transition and no distinct intermediates identified (Figure 5). Native α -LA required the most activation energy to unfold (Figure 5B, top panel). RCM α -LA required less activation energy to induce unfolding (Figure 5B, middle panel). The difference is presumably due to native α -LA having intact disulfide bonds unlike RCM α -LA and possibly the destabilising effect of eight additional negative charges as a result of carboxymethylation. Interestingly, RCM α -LA required a higher activation energy to

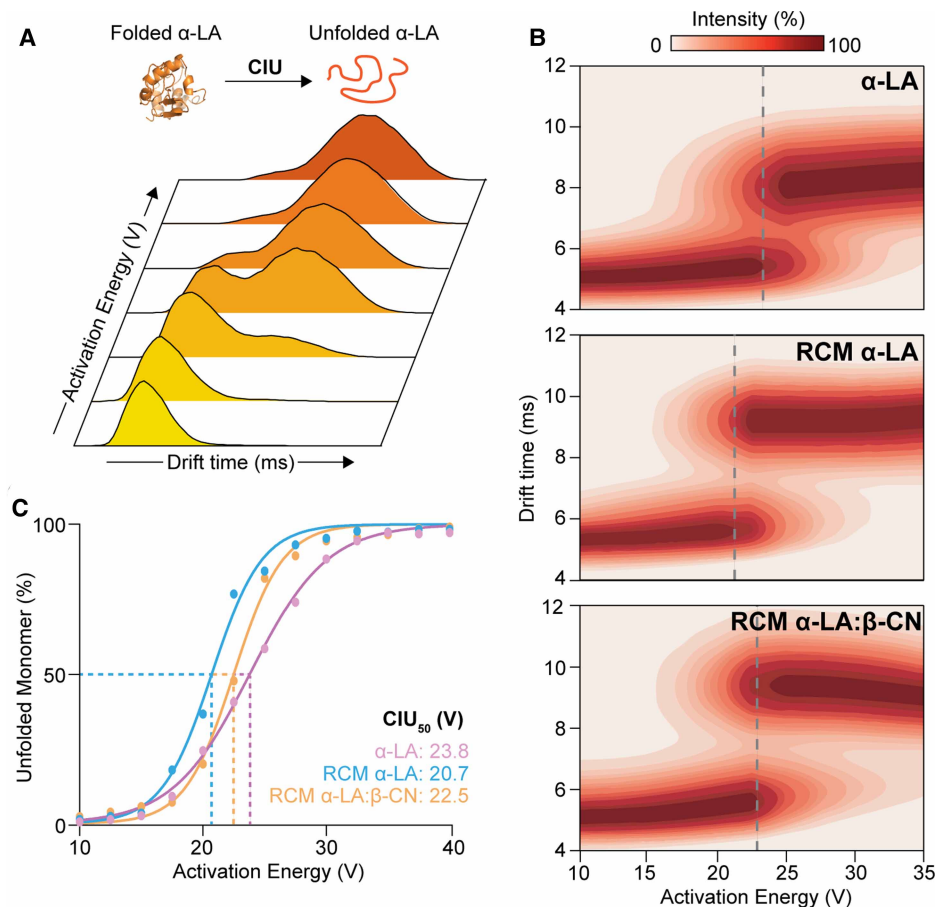


Figure 5. CIU analysis reveals β -CN enhances the stability of RCM α -LA.

(A) Schematic representation of the unfolding dynamics of native α -LA, demonstrating that increasing the gas-phase activation energy promotes the unfolding of α -LA as monitored for the α -LA M^{7+} ions. The gas-phase unfolding pathway comprised only two distinct populations (folded and unfolded) between 10 and 40 V. No additional transitions were observed with activation up to 150 V. (B) CIU heat maps of native α -LA M^{7+} (top panel), RCM α -LA in the absence (middle panel) and presence (bottom panel) of β -CN at a ratio of 2 : 1 (RCM α -LA : β -CN) with a 15 min incubation at 37°C. The single unfolding transition is indicated by grey dashed lines. (C) The abundance of unfolded α -LA M^{7+} was plotted as a function of activation energy for native α -LA (purple), RCM α -LA (blue) and RCM α -LA in the presence of β -CN (orange) at a ratio of 2 : 1 (RCM α -LA : β -CN) with a 15 min incubation in order to assess the stability. Data were fitted with a sigmoidal function and the stability was quantified by calculating the CIU₅₀ (i.e. activation energy at which the abundance of unfolded monomer was 50%, dashed lines).

induce unfolding when in the presence of β -CN compared with RCM α -LA alone (Figure 5B, bottom panel). To quantitatively assess the stability of the various forms of α -LA, the relative populations of folded and unfolded α -LA were plotted as a function of activation energy and the energy required for 50% of α -LA monomer to be unfolded (CIU₅₀) was calculated as a measure of stability (Figure 5C). Native α -LA had a CIU₅₀ of 23.8 V whereas RCM α -LA had a lower CIU₅₀ of 20.7 V (Figure 5C). Moreover, native α -LA unfolded at a slower rate (0.14 ms/V) than RCM α -LA (0.21 ms/V) (Figure 5C). Interestingly, the presence of β -CN increased the CIU₅₀ of RCM α -LA to 22.5 V and restored the rate of unfolding of RCM α -LA to that of RCM α -LA alone (Figure 5C). The data indicate that β -CN interacts with the monomer of RCM α -LA and enhances its stability as a means of preventing amyloid fibril formation.

Discussion

Improved understanding of the structural characteristics which direct proteins along unfolding pathways can inform approaches towards the treatment of protein misfolding diseases. Furthermore, understanding the

molecular basis that underlies molecular chaperone activity to prevent protein unfolding and aggregation can provide additional avenues for therapeutic intervention. Herein, we investigated the effects of the molecular chaperone β -CN on both amorphous and amyloid fibrillar aggregation of α -LA as representative examples of protein unfolding and its mitigation. In a broader context, the study also has relevance to the dairy industry as the chaperone action of β -CN is important in stabilising other milk proteins such as α -LA, for example under ultra-high temperature and pasteurisation processing [22,39].

β -CN inhibits the fibrillar aggregation of RCM α -LA more effectively than DTT α -LA amorphous aggregation (Figure 1B,D) although it has no observable effect on the lag-phase of α -LA aggregation in each case. While β -CN has been previously shown to inhibit both amorphous and fibrillar aggregation of a range of proteins, this is the first instance in which the chaperone activity of β -CN has been assessed against a single, aggregation-prone protein that can form either amorphous or fibrillar aggregates under physiologically relevant conditions (i.e. pH near 7.0 and 37°C) and without the need for harsh conditions or treatments that are not amenable to native MS (typically temperature >45°C, very acidic pH or using organic solvents). In general, molecular chaperones are classified into two classes, namely stabilising ‘holdases’ [40] and energy dependant ‘foldases’. In agreement with previous studies [21–24,41,42], our data are consistent with β -CN functioning as a holdase to prevent protein aggregation without refolding aggregation-prone proteins to their native state.

Intrinsic tryptophan fluorescence and extrinsic bis-ANS fluorescence studies provided insights into the structural differences between α -LA forms (Figure 2A,B). Greater exposed hydrophobicity but near-native levels of tryptophan fluorescence exhibited by DTT α -LA implied a molten globule-like state in which secondary structure is mainly present while a dynamic overall structure exposes hydrophobic regions such as the protein’s core. Conversely, increased tryptophan fluorescence for RCM α -LA indicated a lack of native structure with little exposed, clustered hydrophobicity, consistent with a non-native, relatively unfolded but stable structure as was previously observed by far-UV circular dichroism spectroscopy [15]. Therefore, a relative lack of exposed hydrophobicity for RCM α -LA may be important to promote fibril formation rather than amorphous aggregation, particularly as amorphous aggregates formed at a much faster rate than amyloid fibrils (compare Figure 1A,B).

IM-MS revealed distinct changes in the proportion of a disordered monomeric state of DTT α -LA and RCM α -LA with time (Figure 3), which may explain differences in the unfolding and aggregation pathways for each α -LA form. For RCM α -LA, the disappearance of a disordered species after 2 h of incubation (Figure 3B) leads to the adoption of a more ordered, compact intermediate conformation that is relatively long lived. It is likely this structure does not expose enough hydrophobicity to self-assemble amorphously but, over time, associates in an ordered, fibrillar form. The phenomenon of intrinsically disordered proteins reorganising and gaining structure prior to fibril formation has been observed previously and may be a key step in the formation of amyloid fibrils [43,44]. The opposite occurs for DTT α -LA. The Cys6–Cys120 disulfide bond of native α -LA is highly accessible to solvent and is reduced within 1 s upon the addition of DTT to give the triply disulfide-bonded form of α -LA which is relatively stable and ordered in conformation [17,45]. Complete reduction in the remaining disulfide bonds occurs after ~5 min of incubation with DTT leading to a disordered molten globule conformation of α -LA that aggregates amorphously [17,45]. Analysis by NMR spectroscopy [17,45] reveals freshly incubated RCM α -LA adopts a similar disordered molten globule conformation to fully DTT-reduced α -LA (i.e. prior to its aggregation), consistent with the IM-MS results in Figure 3.

While β -CN forms complexes with other amorphously aggregating proteins to prevent their aggregation (41), β -CN more effectively protects against fibrillar RCM α -LA (Figure 1). Notably, this occurs without HMW complexation and despite the reduced hydrophobicity of RCM α -LA (Figure 2). *In vivo*, β -CN associated with the other caseins (of which there are three in bovine milk) to form the large amorphous aggregate known as the casein micelle [22–24]. Consistent with their intrinsically disordered nature, β -CN and the other caseins adopt a significant proportion of polyproline-II (PP-II) helical secondary structure, mostly within their proline, glutamine-rich regions [22–24]. These regions are involved in casein–casein interactions within the casein micelle and with other proteins during chaperone action [22–24]. Thus, hydrophobicity does not play a large role in protein interactions involving caseins [24], which may contribute to the greater efficiency of β -CN to inhibit α -LA fibril formation compared with α -LA amorphous aggregation, since the latter is dominated by hydrophobic association. From Raman spectroscopic studies, the molten globule state of α -LA at acidic pH adopts significant PP-II helical structure which most likely arises from unfolding of its β -sheet domain [46]. Furthermore, NMR spectroscopy shows that the molten globule state of α -LA present at acidic pH has a very similar conformation to that of RCM α -LA and fully DTT α -LA [45]. The presence of PP-II structure in RCM

α -LA and β -CN, coupled with the prevalence of the PP-II conformation in protein–protein interactions [47], would predispose the PP-II structured regions in both proteins to co-associate, albeit transiently, and hence prevent the conversion of RCM α -LA to the amyloid fibrillar state.

β -CN is also known to undergo post-translational modifications that affect its chaperone activity. It is phosphorylated at five serine residues which form sites for binding calcium phosphate via nanocluster formation [22,41,48,49]. Dephosphorylation of β -CN reduces its chaperone activity against amorphous aggregation of ovotransferrin and apo α -LA, whilst remaining effective against fibril formation of RCM κ -casein [48], implying that electrostatic interactions play some part in β -CN chaperone action against amorphously aggregating proteins but are not involved in regulating chaperone action against fibril-forming proteins. β -CN exhibits very similar chaperone action to α s-casein [20] and sHsps. All are much better chaperones in preventing the aggregation of slowly aggregating proteins [20,50]. Thus, kinetics may also be a factor in the greater chaperone activity of β -CN in preventing RCM α -LA from aggregating, since DTT α -LA aggregates at a much faster rate than RCM α -LA (Figure 1).

We have investigated the heterogeneity, unfolding dynamics and stability of monomeric α -LA using IM-MS. Our data show that RCM α -LA is relatively more unfolded and structurally less stable than the native form (Figures 4 and 5). Interestingly, native and RCM α -LA showed similar ATD features (i.e. centroid and FWHM) (Figure 4B, top panel), suggesting that RCM α -LA exists in a relatively stable off-pathway structure with heterogeneity comparable to that of native α -LA. Upon unfolding (Figure 4B,C, bottom panel), native α -LA showed greater heterogeneity than RCM α -LA, likely due to RCM α -LA already existing in a partially disordered conformation and thereby having fewer conformational options available, whereas native α -LA can exist in all conformations between folded and disordered.

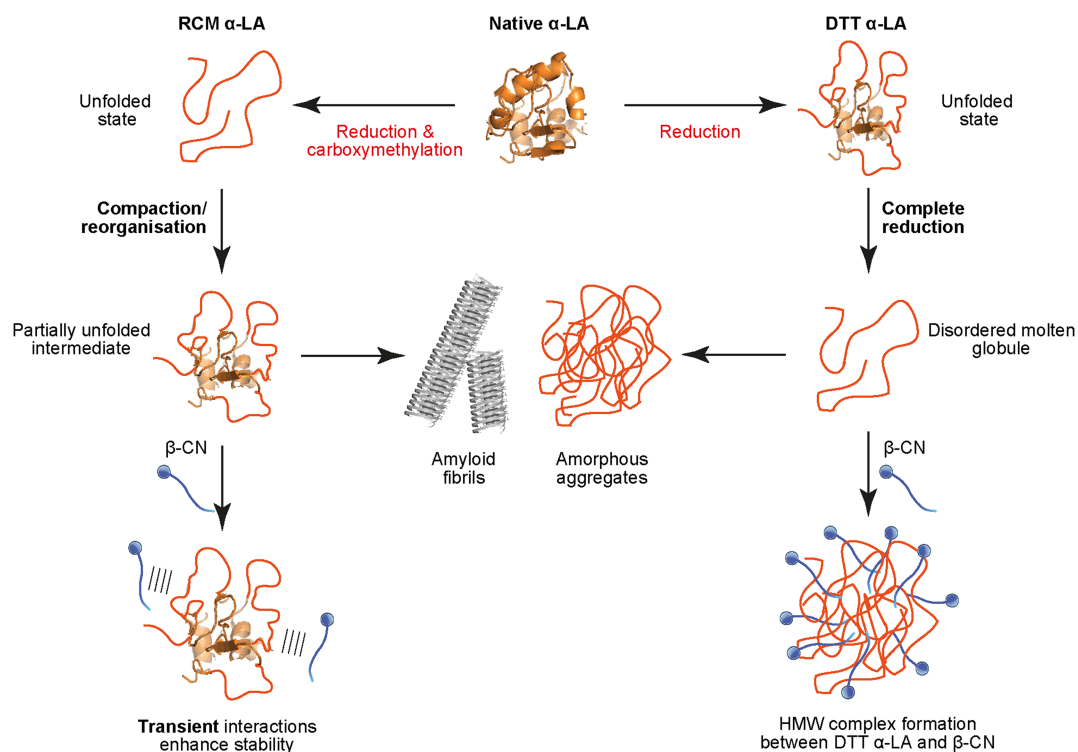


Figure 6. β -CN inhibits the aggregation of α -LA through two distinct mechanisms.

The sequential reduction in α -LA disulfide bonds initiates unfolding and induces an increase in exposed hydrophobicity and self-association to promote amorphous aggregation. The addition of β -CN sequesters disordered, hydrophobic α -LA into a HMW complex to prevent amorphous aggregation. Conversely, the complete reduction and carboxymethylation of α -LA results in the monomer condensing into a semi-stable intermediate with little exposed hydrophobicity which can form amyloid fibrils over time. In this scenario, β -CN interacts transiently with RCM α -LA intermediates to improve monomeric stability and inhibit amyloid fibril formation.

Structural changes from transition states correlate well with changes observed by CIU [38]. We showed that all α -LA forms unfold in a simple two-step mechanism. CIU analysis (Figure 5) also showed that RCM α -LA was more prone to unfolding as all its disulfide bonds are reduced, weakening its tertiary structure. However, the enhanced stability afforded by β -CN reduces the propensity of RCM α -LA to unfold. It appears, therefore, that β -CN inhibits fibril formation via a transient interaction (as confirmed by analytical-SEC, Figure 2) which induces conformational change in RCM α -LA promoting a more stable, native-like structure which is less prone to aggregation. Consistent with this, NMR studies also observed transient interactions between α -crystallin and RCM α -LA [45], whereas stabilisation and eventual complexation occurred between the disordered molten globule state of amorphously aggregating α -LA [17,45]. α s-Casein also prevents the amorphous aggregation of DTT α -LA by complexation, as monitored by NMR spectroscopy [21]. Figure 6 provides a schematic representation of the different mechanisms of β -CN chaperone action with amorphous and amyloid fibrillar aggregating α -LA as elucidated in this study. The mechanisms bear significant similarity to those for the inhibition of amorphous and amyloid fibrillar aggregation by sHsps [51–54].

In summary, DTT and RCM α -LA monomers have different structural properties apparent during the early stages of aggregation, with RCM α -LA displaying compaction to a less hydrophobic, stable intermediate whereas DTT α -LA rapidly unfolds to a molten globule state that exposes hydrophobicity and promotes the association with additional DTT α -LA monomers. These data are consistent with the notion that amorphous aggregation depends on exposing hydrophobicity whilst fibrillar aggregation relies on the formation of a more ordered monomeric intermediate with less exposed hydrophobicity that associates more slowly. While β -CN is able to protect against the amorphous aggregation of DTT α -LA, probably via hydrophobic and electrostatic interactions, a different and more efficient mechanism prevents fibril formation of RCM α -LA which may involve the mutual interaction of PP-II helical regions in both proteins. In doing so, β -CN interacts with RCM α -LA transiently to increase its stability, restricting its capacity to enter the amyloid fibril off-folding pathway (Figure 6). In a general sense, this study has provided insights into the conformational properties which induce amorphous or fibrillar aggregation and the mechanism of chaperone function in proteostasis. Finally, the use of IM-MS and CIU to investigate unfolding protein–chaperone interactions has been demonstrated, affording unique molecular insights compared with other biophysical techniques.

Abbreviations

β -CN, β -casein; ANS, 8-anilino-1-naphthalene-sulfonic acid; ATD, arrival time distribution; CIU, collision-induced dissociation; DTT, dithiothreitol; FWHM, full-width half maximum; HMW, high molecular weight; IM, ion mobility; MS, mass spectrometry; PP-II, polyproline-II; RCM, reduced and carboxymethylated; SEC, size-exclusion chromatography; sHsps, small heat-shock proteins; TEM, transmission electron microscopy; α -LA, α -lactalbumin.

Author Contributions

H.M.S., B.J., J.A.C. and T.L.P. designed the research; H.M.S. performed the experiments; H.M.S., B.J., J.A.C. and T.L.P. analysed experimental data; H.M.S., B.J., J.A.C. and T.L.P. wrote the manuscript.

Funding

This research was financially supported in part by an Australian Research Council Discovery Project Grant to T.L.P. (DP170102033) and a National Health and Medical Research Council Project Grant to J.A.C. (1068087).

Acknowledgements

H.M.S. is supported by a Faculty of Sciences Divisional Scholarship from the University of Adelaide. Many thanks to Michael Graetz for his assistance and expertise in regards to fluorescence and TEM data acquisition. We thank Adelaide Microscopy (University of Adelaide) for TEM technical assistance. We also thank Flinders Analytical (Flinders University, Australia) for access to IM-MS instrumentation. This research was financially supported in part by an Australian Research Council Discovery Project Grant to T.L.P. (DP170102033) and a National Health and Medical Research Council Project Grant to J.A.C. (1068087).

Open Access

Open access for this article was enabled by the participation of University of Adelaide in an all-inclusive *Read & Publish* pilot with Portland Press and the Biochemical Society under a transformative agreement with CAUL.

Competing Interests

The authors declare that there are no competing interests associated with the manuscript.

References

- Dinner, A.R., Šalib, A., Smitha, L.J., Dobson, C.M. and Karplus, M. (2000) Understanding protein folding via free-energy surfaces from theory and experiment. *Trends Biochem. Sci.* **25**, 331–339 [https://doi.org/10.1016/S0968-0004\(00\)01610-8](https://doi.org/10.1016/S0968-0004(00)01610-8)
- Naeem, A., Khan, T.A. and Fazili, N.A. (2015) Protein folding and misfolding: a perspective from theory. *J. Glycom. Lipidom.* **5**, 868–893 <https://doi.org/10.4172/2153-0637.1000128>
- Dobson, C.M. (2004) Principles of protein folding, misfolding and aggregation. *Semin. Cell Dev. Biol.* **15**, 3–16 <https://doi.org/10.1016/j.semdb.2003.12.008>
- Knowles, T.P.J., Vendruscolo, M. and Dobson, C.M. (2014) The amyloid state and its association with protein misfolding diseases. *Nat. Rev. Mol. Cell Biol.* **15**, 384–396 <https://doi.org/10.1038/nrm3810>
- Ecroyd, H. and Carver, J.A. (2008) Unraveling the mysteries of protein folding and misfolding. *IUBMB Life* **60**, 769–774 <https://doi.org/10.1002/iub.117>
- Stranks, S.D., Ecroyd, H., Van Sluyter, S., Waters, E.J., Carver, J.A. and Von Smekal, L. (2009) Model for amorphous aggregation processes. *Phys. Rev. E* **80**, 051907 <https://doi.org/10.1103/PhysRevE.80.051907>
- Kirschner, D.A., Abraham, C. and Selkoe, D.J. (1986) X-ray diffraction from intraneuronal paired helical filaments and extraneuronal amyloid fibers in Alzheimer disease indicates cross-beta conformation. *Proc. Natl Acad. Sci. U.S.A.* **83**, 503–507 <https://doi.org/10.1073/pnas.83.2.503>
- Khurana, R., Ionescu-Zanetti, C., Pope, M., Li, J., Nielson, L., Ramirez-Alvarado, M. et al. (2003) A general model for amyloid fibril assembly based on morphological studies using atomic force microscopy. *Biophys. J.* **85**, 1135–1144 [https://doi.org/10.1016/S0006-3495\(03\)74550-0](https://doi.org/10.1016/S0006-3495(03)74550-0)
- Rochet, J.C. and Lansbury, P.T. (2000) Amyloid fibrillogenesis: themes and variations. *Curr. Opin. Struct. Biol.* **10**, 60–68 [https://doi.org/10.1016/S0959-440X\(99\)00049-4](https://doi.org/10.1016/S0959-440X(99)00049-4)
- Uversky, V.N. and Fink, A.L. (2006) Protein misfolding, aggregation, and conformational diseases. *Protein Rev.* **4**, 450 <https://doi.org/10.1007/978-0-387-36534-3>
- Soto, C. (2003) Unfolding the role of protein misfolding in neurodegenerative diseases. *Nat. Rev. Neurosci.* **4**, 49–60 <https://doi.org/10.1038/nrn1007>
- Truscott, R.J.W. (2005) Age-related nuclear cataract - oxidation is the key. *Exp. Eye Res.* **80**, 709–725 <https://doi.org/10.1016/j.exer.2004.12.007>
- Permyakov, E.A. and Berliner, L.J. (2000) α -Lactalbumin: structure and function. *FEBS Lett.* **473**, 269–274 [https://doi.org/10.1016/S0014-5793\(00\)01546-5](https://doi.org/10.1016/S0014-5793(00)01546-5)
- Acharya, K.R., Ren, J.S., Stuart, D.I., Phillips, D.C. and Fenna, R.E. (1991) Crystal structure of human α -lactalbumin at 1.7 Å resolution. *J. Mol. Biol.* **221**, 571–581 [https://doi.org/10.1016/0022-2836\(91\)80073-4](https://doi.org/10.1016/0022-2836(91)80073-4)
- Kulig, M. and Ecroyd, H. (2012) The small heat-shock protein α B-crystallin uses different mechanisms of chaperone action to prevent the amorphous versus fibrillar aggregation of α -lactalbumin. *Biochem. J.* **448**, 343–352 <https://doi.org/10.1042/BJ20121187>
- Goers, J., Permyakov, S.E., Permyakov, E.A., Uversky, V.N. and Fink, A.L. (2002) Conformational prerequisites for α -lactalbumin fibrillation. *Biochemistry* **41**, 12546–12551 <https://doi.org/10.1021/bi0262698>
- Carver, J.A., Lindner, R.A., Lyon, C., Canet, D., Hernandez, H., Dobson, C.M. et al. (2002) The interaction of the molecular chaperone α -crystallin with unfolding α -lactalbumin: a structural and kinetic spectroscopic study. *J. Mol. Biol.* **318**, 815–827 [https://doi.org/10.1016/S0022-2836\(02\)00144-4](https://doi.org/10.1016/S0022-2836(02)00144-4)
- Bornhoff, G., Sloan, K., McLain, C., Gogol, E.P. and Fisher, M.T. (2006) The effects of the flavonoid baicalein and osmolytes on the Mg²⁺ accelerated aggregation/fibrillation of carboxymethylated bovine 1SS- α -lactalbumin. *Arch. Biochem. Biophys.* **453**, 75–86 <https://doi.org/10.1016/j.abb.2006.02.001>
- Farrell, J., Wickham, E.D., Unruh, J.J., Qi, P.X. and Hoagland, P.D. (2001) Secondary structural studies of bovine caseins: temperature dependence of β -casein structure as analyzed by circular dichroism and FTIR spectroscopy and correlation with micellization. *Food Hydrocoll.* **15**, 341–354 [https://doi.org/10.1016/S0268-005X\(01\)00080-7](https://doi.org/10.1016/S0268-005X(01)00080-7)
- Cragnell, C., Choi, J., Segad, M., Lee, S., Nilsson, L. and Skepö, M. (2017) Bovine β -casein has a polydisperse distribution of equilibrium micelles. *Food Hydrocoll.* **70**, 65–68 <https://doi.org/10.1016/j.foodhyd.2017.03.021>
- Morgan, P.E., Treweek, T.M., Lindner, R.A., Price, W.E. and Carver, J.A. (2005) Casein proteins as molecular chaperones. *J. Agric. Food Chem.* **53**, 2670–2683 <https://doi.org/10.1021/jf048329h>
- Holt, C., Carver, J.A., Ecroyd, H. and Thorn, D.C. (2013) Invited review: Caseins and the casein micelle: their biological functions, structures, and behavior in foods. *J. Dairy Sci.* **96**, 6127–6146 <https://doi.org/10.3168/jds.2013-6831>
- Thorn, D.C., Ecroyd, H., Carver, J.A. and Holt, C. (2015) Casein structures in the context of unfolded proteins. *Int. Dairy J.* **46**, 2–11 <https://doi.org/10.1016/j.idairyj.2014.07.008>
- Holt, C., Raynes, J.K. and Carver, J.A. (2019) Sequence characteristics responsible for protein–protein interactions in the intrinsically disordered regions of caseins, amelogenins, and small heat-shock proteins. *Biopolymers* **110**, e23319 <https://doi.org/10.1002/bip.23319>
- Williams, D.M. and Pukala, T.L. (2013) Novel insights into protein misfolding diseases revealed by ion mobility-mass spectrometry. *Mass Spectrom. Rev.* **32**, 169–187 <https://doi.org/10.1002/mas.21358>
- Politis, A., Stengel, F., Hall, Z., Hernández, H., Leitner, A., Walzthoeni, T. et al. (2014) A mass spectrometry-based hybrid method for structural modeling of protein complexes. *Nat. Methods* **11**, 403–406 <https://doi.org/10.1038/nmeth.2841>
- Sharon, M. and Robinson, C.V. (2007) The role of mass spectrometry in structure elucidation of dynamic protein complexes. *Annu. Rev. Biochem.* **76**, 167–193 <https://doi.org/10.1146/annurev.biochem.76.061005.090816>
- Dixit, S.M., Polasky, D.A. and Ruotolo, B.T. (2018) Collision induced unfolding of isolated proteins in the gas phase: past, present, and future. *Curr. Opin. Chem. Biol.* **42**, 93–100 <https://doi.org/10.1016/j.cbpa.2017.11.010>
- Rabuck-Gibbons, J.N., Lodge, J.M., Mapp, A.K. and Ruotolo, B.T. (2019) Collision-induced unfolding reveals unique fingerprints for remote protein interaction sites in the KIX regulation domain. *J. Am. Soc. Mass Spectrom.* **30**, 94–102 <https://doi.org/10.1007/s13361-018-2043-6>
- Shechter, Y., Patchornik, A. and Burstein, Y. (1973) Selective reduction of cystine I–VIII in α -lactalbumin of bovine milk. *Biochemistry* **12**, 3407–3413 <https://doi.org/10.1021/bi00742a007>
- Ecroyd, H. and Carver, J.A. (2008) The effect of small molecules in modulating the chaperone activity of α B-crystallin against ordered and disordered protein aggregation. *FEBS J.* **275**, 935–947 <https://doi.org/10.1111/j.1742-4658.2008.06257.x>

- 32 Carver, J.A., Duggan, P.J., Ecroyd, H., Liu, Y., Meyer, A.G. and Tranberg, C.E. (2010) Carboxymethylated- κ -casein: a convenient tool for the identification of polyphenolic inhibitors of amyloid fibril formation. *Bioorgan. Med. Chem.* **18**, 222–228 <https://doi.org/10.1016/j.bmc.2009.10.063>
- 33 Liu, Y., Jovceviski, B. and Pukala, T.L. (2019) C-phycocyanin from spirulina inhibits α -synuclein and amyloid- β fibril formation but not amorphous aggregation. *J. Nat. Prod.* **82**, 66–73 <https://doi.org/10.1021/acs.jnatprod.8b00610>
- 34 Eschweiler, J.D., Rabuck-Gibbons, J.N., Tian, Y. and Ruotolo, B.T. (2015) CIUSuite: a quantitative analysis package for collision induced unfolding measurements of gas-phase protein ions. *Anal. Chem.* **87**, 11516–11522 <https://doi.org/10.1021/acs.analchem.5b03292>
- 35 Jovceviski, B., Kelly, M.A., Aquilina, J.A., Benesch, J.L.P. and Ecroyd, H. (2017) Evaluating the effect of phosphorylation on the structure and dynamics of hsp27 dimers by means of ion mobility mass spectrometry. *Anal. Chem.* **89**, 13275–13282 <https://doi.org/10.1021/acs.analchem.7b03328>
- 36 Ewbank, J.J. and Creighton, T.E. (1993) Structural characterization of the disulfide folding intermediates of bovine α -lactalbumin. *Biochemistry* **32**, 3694–3707 <https://doi.org/10.1021/bi00065a023>
- 37 Konermann, L., Ahadi, E., Rodriguez, A.D. and Vahidi, S. (2013) Unraveling the mechanism of electrospray ionization. *Anal. Chem.* **85**, 2–9 <https://doi.org/10.1021/ac302789c>
- 38 Zhong, Y., Han, L. and Ruotolo, B.T. (2014) Collisional and coulombic unfolding of gas-phase proteins: high correlation to their domain structures in solution. *Angew. Chem. Int. Ed.* **53**, 9209–9212 <https://doi.org/10.1002/anie.201403784>
- 39 Raynes, J.K., Day, L., Augustin, M.A. and Carver, J.A. (2015) Structural differences between bovine A1 and A2 β -casein alter micelle self-assembly and influence molecular chaperone activity. *J. Dairy Sci.* **98**, 2172–2182 <https://doi.org/10.3168/jds.2014-8800>
- 40 Gregersen, N., Bross, P., Vang, S. and Christensen, J.H. (2006) Protein misfolding and human disease. *Annu. Rev. Genomics Hum. Genet.* **7**, 103–124 <https://doi.org/10.1146/annurev.genom.7.080505.115737>
- 41 Carver, J.A., Ecroyd, H., Truscott, R.J.W., Thorn, D.C. and Holt, C. (2018) Proteostasis and the regulation of intra- and extracellular protein aggregation by ATP-independent molecular chaperones: lens α -crystallins and milk caseins. *Acc. Chem. Res.* **51**, 745–752 <https://doi.org/10.1021/acs.accounts.7b00250>
- 42 Zhang, X., Fu, X., Zhang, H., Liu, C., Jiao, W. and Chang, Z. (2005) Chaperone-like activity of β -casein. *Int. J. Biochem. Cell Biol.* **37**, 1232–1240 <https://doi.org/10.1016/j.biocel.2004.12.004>
- 43 Das, S., Pukala, T.L. and Smid, S.D. (2018) Exploring the structural diversity in inhibitors of α -synuclein amyloidogenic folding, aggregation, and neurotoxicity. *Front. Chem.* **6**, 181 <https://doi.org/10.3389/fchem.2018.00181>
- 44 Pavlova, A., Cheng, C.-Y., Kinnebrew, M., Lew, J., Dahlquist, F.W. and Han, S. (2016) Protein structural and surface water rearrangement constitute major events in the earliest aggregation stages of tau. *Proc. Natl. Acad. Sci. U.S.A.* **113**, E127–E136 <https://doi.org/10.1073/pnas.1504415113>
- 45 Lindner, R.A., Kapur, A. and Carver, J.A. (1997) The interaction of the molecular chaperone, α -crystallin, with molten globule states of bovine α -lactalbumin. *J. Biol. Chem.* **272**, 27722–27729 <https://doi.org/10.1074/jbc.272.44.27722>
- 46 Ashton, L. and Blanch, E.W. (2010) pH-induced conformational transitions in α -lactalbumin investigated with two-dimensional Raman correlation variance plots and moving windows. *J. Mol. Struct.* **974**, 132–138 <https://doi.org/10.1016/j.molstruc.2010.03.005>
- 47 Adzhubei, A.A., Sternberg, M.J.E. and Makarov, A.A. (2013) Polyproline-II helix in proteins: structure and function. *J. Mol. Biol.* **425**, 2100–2132 <https://doi.org/10.1016/j.jmb.2013.03.018>
- 48 Koudelka, T., Hoffmann, P. and Carver, J.A. (2009) Dephosphorylation of α S- and β -caseins and its effect on chaperone activity: a structural and functional investigation. *J. Agric. Food Chem.* **57**, 5956–5964 <https://doi.org/10.1021/jf9008372>
- 49 Holt, C. and Carver, J.A. (2012) Darwinian transformation of a “scarcely nutritious fluid” into milk. *J. Evol. Biol.* **25**, 1253–1263 <https://doi.org/10.1111/j.1420-9101.2012.02509.x>
- 50 Cox, D., Selig, E., Griffin, M.D.W., Carver, J.A. and Ecroyd, H. (2016) Small heat-shock proteins prevent α -synuclein aggregation via transient interactions and their efficacy is affected by the rate of aggregation. *J. Biol. Chem.* **291**, 22618–22629 <https://doi.org/10.1074/jbc.M116.739250>
- 51 Esposito, G., Garvey, M., Alverdi, V., Pettrossi, F., Corazza, A., Fogolari, F., et al. (2013) Monitoring the interaction between β 2-microglobulin and the molecular chaperone α B-crystallin by NMR and mass spectrometry: α B-crystallin dissociates β 2-microglobulin oligomers. *J. Biol. Chem.* **288**, 17844–17858 <https://doi.org/10.1074/jbc.M112.448639>
- 52 Cox, D., Carver, J.A. and Ecroyd, H. (2014) Preventing α -synuclein aggregation: the role of the small heat-shock molecular chaperone proteins. *Biochim. Biophys. Acta* **1842**, 1830–1843 <https://doi.org/10.1016/j.bbadis.2014.06.024>
- 53 Treweek, T.M., Meehan, S., Ecroyd, H. and Carver, J.A. (2015) Small heat-shock proteins: important players in regulating cellular proteostasis. *Cell. Mol. Life Sci.* **72**, 429–451 <https://doi.org/10.1007/s00018-014-1754-5>
- 54 Carver, J.A., Grosas, A.B., Ecroyd, H. and Quinlan, R.A. (2017) The functional roles of the unstructured N- and C-terminal regions in α B-crystallin and other mammalian small heat-shock proteins. *Cell Stress Chaperones* **22**, 627–638 <https://doi.org/10.1007/s12192-017-0789-6>